Magnetite Accelerated Stress Corrosion Cracking of Ni-based Alloys in PbO-Containing Water

Won-Ik Choi[a,b], Geun Dong Song[a], Soon-Hyeok Jeon[a], Sun Jin Kim[b], Do Haeng Hur[a,*]

[a] Nuclear Materials Research Division, Korea Atomic Energy Research Institute, 989-111 Daedeok-daero, Yuseong-gu, Daejeon 34057, Republic of Korea
[b] Division of Materials Science and Engineering, Hanyang University, 222 Wangsimni-ro, Seongdong-gu, Seoul, 04763, Republic of Korea
[*]Corresponding author: dhhur@kaeri.re.kr

1. Introduction

Ni-based alloys such as Alloy 600 and Alloy 690 are used as steam generator tube materials in pressurized water reactor (PWR). However, Alloy 600 tubing has been susceptible to several types of corrosion degradation: stress corrosion cracking (SCC) in both primary and secondary water, pitting and intergranular attack in secondary water. Therefore, Alloy 600 has been replaced with thermally treated Alloy 690, which contains 29-31 wt% Cr. Alloy 690 tubes have not experienced any corrosion related damages since their first application to steam generators in 1987.

Extensive studies on secondary side deterioration have been carried out to confirm that corrosion of Alloy 600 is accelerated in various impurity-containing solutions and pH conditions [1, 2]. However, most of these studies have been performed under unrealistically strong conditions. Above all things, we should keep in mind that tubes and crevices in the operating steam generators are covered with deposits. The deposits are porous and mainly consist of magnetite, which is the corrosion products produced in carbon steel piping due to flow accelerated corrosion [3]. This means that real corrosion phenomena occur on the surfaces of tubes covered with porous magnetite, not on the directly exposed tube surfaces to the bulk water. Therefore, the effects of the magnetite deposits should be considered when evaluating the corrosion behavior of the steam generator tube materials.

Recently, we have reported that the galvanic effect between Ni-based alloys and magnetite in a variety of environments significantly accelerates general corrosion of the Ni-based alloys [4-6]. Therefore, it is necessary to expand the study to the area of stress corrosion cracking, which is the main corrosion phenomenon of Ni-based alloys. This paper presents the effect of magnetite on the stress corrosion cracking behavior and the properties of the oxide film of Ni-based alloys in 100 ppm PbO-containing solution. PbO was selected as an impurity in the simulated secondary environments, because lead compounds are known to accelerate stress corrosion cracking of Ni-based alloys [7]

2. Experimental Methods

2.1 Preparation of magnetite deposited SCC specimens

Alloy 600 MA, 600 TT, and 690 TT were used as test materials. Rectangular sheets with a dimension of 7 mm $\times$ 24.4 mm $\times$ 1.25 mm were ground using silicon carbide papers down to #1000 grits, and then ultrasonically cleaned in acetone. These sheets were bended in a U-shape with an inner radius of 2.67 mm. After bending, the legs of the specimen were fastened to be parallel to each other using a bolt and nut made of Alloy 600 material. The total strain on the angular outside surface of the assembled U-bend specimen was estimated to be approximately 28% by measurement of dimensional change.

To evaluate the effect of magnetite on the SCC behavior of Alloy 600, an SCC specimen should be in contact with magnetite in a test solution. To make this condition, magnetite layer was electrodeposited on the whole surface of the assembled U-bend specimen except the apex area of about 0.8 mm width in a deposition solution. Details for the electrodeposition technique of magnetite are given elsewhere [4-6, 8].

2.2 SCC test

SCC tests were conducted in static Ni-autoclaves with a capacity of 3.8 L. Magnetite-free U-bend specimens were located on a specimen holder made of Alloy 600 material. Magnetite deposited U-bend specimens were located on a magnetite-electrodeposited Alloy 600 holder to avoid any galvanic corrosion between the specimens and holder. These two types of SCC specimens were loaded in a separated autoclave but with the same condition.

The SCC tests were conducted in simulated secondary water containing 100 ppm PbO in weight at 315°C. This solution was prepared by adjusting the pH of deionized water to 9.0 at 25°C using NaOH. Finally, PbO of 100 ppm was added to the solution. The added PbO was not completely dissolved even by stirring the solution for 10 min and the solution pH was not changed by addition of PbO at 25°C.

The autoclave operation was stopped to examine the U-bend specimens after a period of 350 h, 650 h, and 1000 h, respectively. The test solution was refreshed and deaerated whenever the autoclave was closed after inspection of the test specimens.

2.3 Crack examination and oxide film analysis

The U-bend specimens were destructively examined to measure the depth and morphology of stress corrosion cracks. TEM specimens including the outer surfaces and cracks were prepared using the FIB. TEM images and elemental compositions of oxides were then analyzed using energy dispersive X-ray spectroscopy (EDS). The chemical states of surface films were analyzed using X-ray photoelectron spectroscopy (XPS).

3. Results and Discussion

Fig. 1 shows the stress corrosion cracks in Alloy 600 MA and Alloy 600 TT after a 650-h test. In both alloys, the uncoupled specimens cracked at the apex region, and the coupled specimen cracked at the interface between the magnetite and exposed specimen. In the case of Alloy 690 TT, no cracks were observed up to 3000 h.
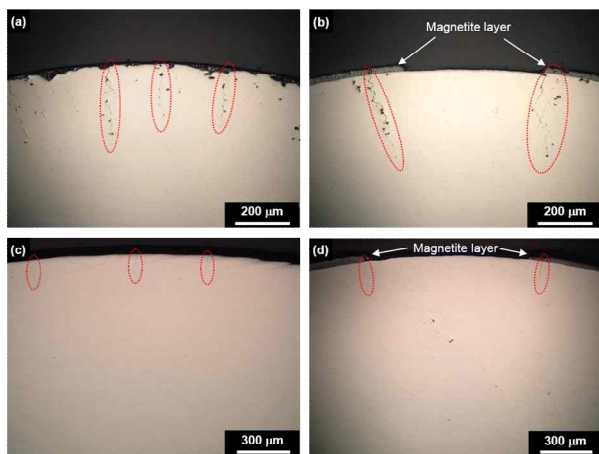
Fig. 1. Stress corrosion cracks in Alloy 600 MA and Alloy 600 TT after a 650-h test: (a) Alloy 600 MA uncoupled, (b) Alloy 600 MA coupled with magnetite, (c) Alloy 600 TT uncoupled, and (d) Alloy 600 TT coupled with magnetite.

Fig. 2 shows the change of the maximum crack depths with exposure time. The maximum crack depths were measured from two or three specimens for each condition. In both Alloy 600 MA and Alloy 600 TT specimens, the coupled specimens with magnetite always revealed deeper crack depths than the uncoupled specimens. Alloy 600 MA specimens coupled with magnetite produced stress corrosion cracks approximately 19 ~ 67% deeper than uncoupled specimens. Alloy 600 TT coupled with magnetite also produced approximately 21 ~ 49% deeper cracks than uncoupled specimens. When comparing the materials of Alloy 600 MA and 600 TT, the average crack depths of Alloy 600 MA were approximately 63% deeper than those of Alloy 600 TT, regardless of magnetite deposit. This means that SCC is accelerated by the magnetite deposit and the magnetite accelerated SCC occurs in not

only Alloy 600 MA but also Alloy 600 TT. However, no SCC was observed in Alloy 690 TT even after a 3000-h exposure.
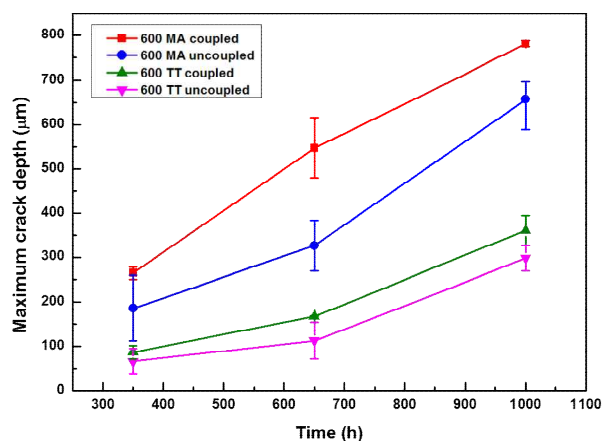
Fig. 2. Evolution of the maximum crack depths in Alloy 600 MA and Alloy 600 TT with testing time in water with 100 ppm PbO.
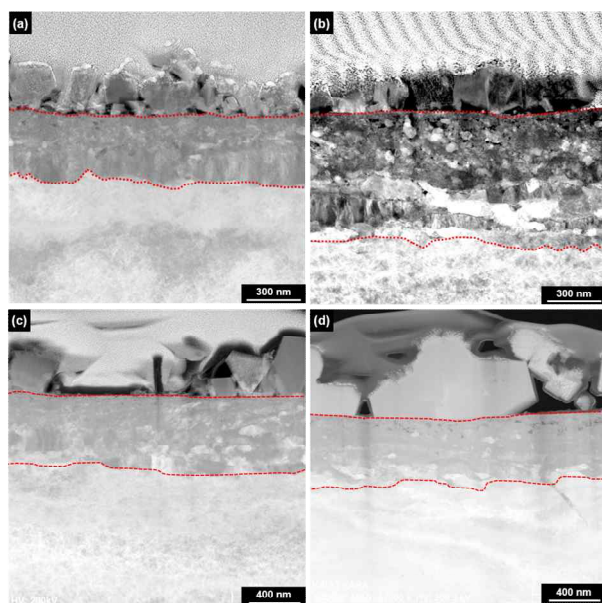
Fig. 3. STEM images on the cross section of the U-bend specimens after a 650-h test: (a) Alloy 600 MA uncoupled, (b) Alloy 600 MA coupled, (c) Alloy 600 TT uncoupled, and (d) Alloy 600 TT coupled.

Fig. 3 shows the STEM photographs of the oxide layers on Alloy 600 MA and Alloy 600 TT. The thickness of the inner oxide layer on the coupled specimen was about twice as thick as that on the uncoupled specimen. Alloy 600 MA showed thicker oxide than Alloy 600 TT. The thick oxide formation on the uncoupled specimen indicates that the corrosion process is stimulated by the deposited magnetite.

Fig. 4 shows TEM-EDS analysis of Alloy 600 MA coupled with magnetite. The particles on the outer surface were NiO and the inner layer beneath the particles was (Cr-Fe) rich and Ni-depleted. This result

together with the thick oxide formation indicates that Ni dissolution from the matrix was accelerated by the magnetite deposit. High Pb content was still detected even at the interface between the inner oxide layer and alloy matrix of the coupled specimen, contrary to the uncoupled specimen. This can be strong evidence for the defective film on the coupled specimens, which facilitate Pb penetration through the film. These processes not only delay the formation of passive film but also deteriorate the protectiveness of the oxide film, resulting in a fast stress corrosion cracking.
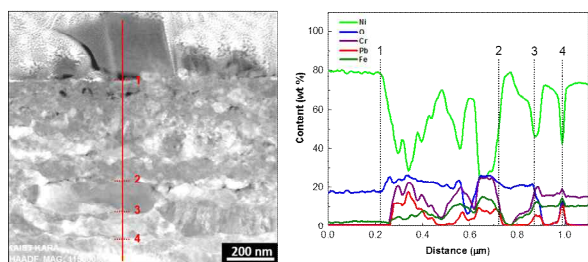
Fig. 4. STEM image and EDS line profile on the cross section near the apex region of the Alloy 600 MA coupled specimen after a 650-h test.

4. Conclusions

1) In both Alloy 600 MA and 600 TT, the coupled specimens with magnetite always produced deeper crack depths than the uncoupled specimens.

2) Magnetite coupled with Alloy 600 MA and Alloy 600 TT accelerated Ni dissolution and formation of a defective thick oxide layer, leading to an accelerated stress corrosion cracking.

3) SCC resistance in this test condition increased in the order: Alloy 600 MA, 600 TT, and 690 TT.

4) Magnetite accelerated stress corrosion cracking phenomena should be considered as an important factor for the SCC mechanism in steam generator tubes in the secondary environments.

Acknowledgement

REFERENCES

[1] J. R. Crum, Stress Corrosion Cracking Testing of Inconel Alloys 600 and 690 under High-Temperature Caustic Conditions, Corrosion, Vol. 42, No. 6, pp. 368-372, 1986.

[2] I.J Yang, Effect of Sulphate and Chloride Ions on the Crevice Chemistry and Stress Corrosion Cracking of Alloy 600 in High Temperature Aqueous Solutions, Corrosion Science, Vol. 33, No. 1, pp. 25-37, 1992.

[3] M.P. Manahan, Mechanical behavior of magnetite from the Oconee-2 and TMI-1 steam generators using miniaturized specimen technology, J. Materials Science, Vol. 25, No. 8, pp. 3415-3423, 1990.

[4] S.H. Jeon, G.D. Song, D.H. Hur, Corrosion Behavior of Alloy 600 Coupled with Electrodeposited Magnetite in Simulated Secondary Water of PWRs, Materials Transactions, Vol. 56, No. 12, pp. 2078-2083, 2015.

[5] S.H. Jeon, G.D. Song, D.H. Hur, Galvanic Corrosion between Alloy 690 and Magnetite in Alkaline Aqueous Solutions, Metals, Vol. 5, No. 4, pp. 2372-2382, 2015.

[6] G.D. Song, S.H Jeon, J.G. Kim, D.H. Hur, Synergistic Effect of Chloride Ions and Magnetite on the Corrosion of Alloy 690 in Alkaline Solution, Corrosion, Vol. 73, No. 3, pp. 216-220, 2017.

[7] H. Takamatsu, B.P. Miglin, P.A. Sherburne, K. Aoki, Study on Lead-Induce Stress Corrosion Cracking of Steam Generator Tubing under AVT Water Chemistry Conditions, Proceedings of Eighth International Symposium on Environmental Degradation of Materials in Nuclear Power System – Water Reactors, Amelia Island, FL, TMS, pp. 216-223, 1997.

[8] C. Goujon, T. Pauporte, C. Mansour, S. Delaunay, and J-L. Bretelle, Electrochemical deposition of thick iron oxide films on nickel based superalloy substrates, Electrochimica Acta, Vol. 176, pp. 230-239, 2015.